

in which the valence and conduction bands enter symmetrically.

- <sup>1</sup>W. Weber, Phys. Rev. Lett. **33**, 371 (1974).  
<sup>2</sup>J. C. Phillips, Phys. Rev. **166**, 832 (1968).  
<sup>3</sup>N. Bloembergen and T. J. Rowland, Phys. Rev. **97**, 1679 (1955).  
<sup>4</sup>W. A. Harrison and S. Ciraci, Phys. Rev. B **10**, 1516 (1974).

\*Work supported by the U. S. Army Research Office.

## Some Comments on the Plasmon Spectrum of Tetrathiafulvalene Tetracyano-*p*-quinodimethane (TTF-TCNQ)\*

P. F. Williams

*Bell Laboratories, Murray Hill, New Jersey 07974, and  
Department of Physics, University of Puerto Rico, Río Piedras, Puerto Rico 00931*

and

A. N. Bloch†

*Department of Chemistry, The Johns Hopkins University, Baltimore, Maryland 21218  
(Received 3 September 1975)*

Our random-phase-approximation model calculation of the high-frequency dielectric response of a quasi-one-dimensional metal is generalized to the case of  $n$  conducting strands per unit cell. For a model of the two-band system tetrathiafulvalene tetracyano-*p*-quinodimethane we obtain good agreement with recent experiments, and also predict an acoustic-plasmon branch. Some implications for the physics of the material are discussed.

The first experimental determination of the plasmon spectrum in a quasi-one-dimensional conductor has recently been reported by Ritsko *et al.*<sup>1</sup> They found that the organic metal tetrathiafulvalene tetracyano-*p*-quinodimethane (TTF-TCNQ)<sup>2</sup> displays an unusual plasmon response qualitatively consistent with the predictions of our model calculation<sup>3</sup> for a simple quasi-one-dimensional metal in the random-phase approximation (RPA). The predictions include negative dispersion, the absence of Landau damping, and a strongly angle-dependent long-wavelength plasma frequency. Our model, however, was not designed to represent a two-band system such as TTF-TCNQ,<sup>4-6</sup> and detailed agreement with experiment was lacking.

Here we extend our calculation to a two-band model more nearly representative of TTF-TCNQ. We find that much of the discrepancy between theory and experiment is removed, and that comparison of the two provides fresh insight into the electronic structure and optical properties of the material. Further, our analysis predicts a sec-

ond, low-frequency plasmon branch, acoustic in the limit of zero interchain bandwidth and experimentally significant at short wavelengths.

The model of Ref. 3 consisted of a periodic array of parallel, infinite, metallic strands, embedded in a uniform medium of dispersionless dielectric constant  $\epsilon_\infty$ , and coupled to one another only by their mutual Coulomb interaction. As we remarked in Ref. 3, the model in this simple form does not apply directly to a material such as TTF-TCNQ, whose crystal structure consists of four conducting chains (two each of stacked TTF and TCNQ molecular ions) per cross-sectional unit cell.<sup>7</sup> To treat such cases, we generalize the model to include  $n$  distinguishable strands per unit cell.

Our analysis proceeds in parallel with our original work,<sup>3</sup> and employs essentially the same notation. If  $\chi_j(q, \Omega)$  [Ref. 3, Eq. (6)] is the complex density-density response function<sup>8</sup> and  $\beta_j(\vec{Q})$  [Ref. 3, Eq. (3)] the molecular form factor for conduction electrons on the  $j$ th strand of the unit cell, the total potential due to an applied potential  $V_{\text{ext}}(\vec{Q})$  is

$$V_{\text{tot}}(\vec{Q}) = \frac{1}{\epsilon_\infty} \left[ V_{\text{ext}}(\vec{Q}) - \frac{4\pi e^2}{Q^2} \sum_{j=1}^n \chi_j(q, \Omega) \beta_j(\vec{Q}) S_j(\vec{Q}) \right]. \quad (1)$$

Equation (1) replaces Eq. (5) of Ref. 3, and we have defined

$$S_j(\vec{Q}) \equiv \sum_{\vec{G}} \beta_j^*(\vec{Q} + \vec{G}) V_{\text{tot}}(\vec{Q} + \vec{G}). \quad (2)$$

The relations (1) and (2) represent an infinite set of coupled linear equations in  $V_{\text{tot}}(\vec{Q})$ ,  $V_{\text{tot}}(\vec{Q} + \vec{G})$ , . . . We multiply these by  $\beta_i^*(\vec{Q} + \vec{G}')$  and sum over all  $\vec{G}'$  to obtain

$$\sum_{j=1}^n [\delta_{ij} + \chi_j(q, \Omega)_{ij}(\vec{Q})] S_j(\vec{Q}) = \frac{1}{\epsilon_\infty} \sum_{\vec{G}} \beta_i^*(\vec{Q} + \vec{G}) V_{\text{ext}}(\vec{Q} + \vec{G}), \quad (3)$$

where the effective interchain Coulomb interaction is [cf. Eq. (7a) of Ref. 3]

$$U_{ij}(\vec{Q}) = (4\pi e^2 / \epsilon_\infty) \sum_{\vec{G}} \beta_i^*(\vec{Q} + \vec{G}) \beta_j(\vec{Q} + \vec{G}) |\vec{Q} + \vec{G}|^{-2}. \quad (4)$$

The inverse dielectric tensor components  $\epsilon^{-1}(\vec{Q} + \vec{G}, \vec{Q}_0 + \vec{G}_0, \Omega)$  can be found by solving (3) for the  $S_j$  and substituting into (1). To determine the plasmon spectrum, however, we need only note that at a plasmon pole, the response to an infinitesimal driving force is finite, so that the plasmon dispersion is completely specified by the zeros of the  $n \times n$  secular determinant:

$$\Delta_n(\vec{Q}, \Omega) \equiv \det[\delta_{ij} + \chi_j(q, \Omega) U_{ij}(\vec{Q})] = 0. \quad (5)$$

We now consider the particular case of TTF-TCNQ. For the moment we neglect the small interchain bandwidths,<sup>5</sup> as in Ref. 3. In this limit the one-electron band structure<sup>5,6</sup> contains two doubly degenerate one-dimensional conduction bands chemically constrained to cross at the Fermi level, and the response function  $\chi_j(q, \Omega)$  for each is of the one-dimensional tight-binding form [Ref. 3, Eq. (11)]. As in Ref. 3, we find it convenient and sufficiently accurate to approximate the form factors  $\beta_j$  by representing the molecular orbitals as anisotropic Gaussians centered at the appropriate lattice sites.<sup>7</sup> With these approximations, the distinction between crystallographically inequivalent chains of like molecules becomes academic, and the plasmon problem reduces to the case  $n = 2$ .

We have solved Eq. (5) numerically for two angles of plasmon propagation,  $\theta$ , relative to the conducting  $b$  axis. Our results for  $\vec{Q}$  in the crystallographic  $a$ - $b$  plane<sup>7</sup> are compared with experiment in Fig. 1; results for the  $b$ - $c^*$  plane are similar. Here we have employed the known cell constants<sup>7</sup>  $a, b, \frac{1}{2}c^*$  and Fermi wave number<sup>9</sup>  $k_F = 0.28\pi/b$ , and have chosen Gaussian orbital radii ( $\rho_{ja}, \rho_{jb}, \rho_{jc^*}$ ) of 2.5, 1.8, 3.5 Å for TCNQ and 2.0, 1.8, 2.0 Å for TTF, consistent with the extent of molecular charge distributions.<sup>5</sup> Since neither  $\epsilon_\infty$  nor the bandwidths  $W_1$  and  $W_2$  are accurately known, they were regarded as adjustable over a range consistent with recent calculations.<sup>5</sup> The final values  $W_1 = 0.4$  eV,  $W_2 = 0.2$  eV,  $\epsilon_\infty = 1.5$  were chosen so as to reproduce the long-wavelength plasma frequency at  $\theta = 0^\circ$  and to give a good fit to experiment elsewhere. This fit is by no means unique, and we regard Fig. 1 as il-

lustrative.

In addition to the usual optic branch, a second, acoustic-plasmon mode appears in Fig. 1. The sole condition for its occurrence when  $n = 2$  is that the two Fermi velocities,  $v_{F1}$  and  $v_{F2}$ , be unequal. Thus the prediction of an acoustic branch is more general for the quasi-one-dimensional case than for isotropic<sup>10</sup> two-band systems.

The presence of a plasmon pole in the very-low-frequency inverse dielectric tensor can have important effects upon the strengths of BCS<sup>10</sup> or Peierls<sup>11</sup> interactions. We note, however, that interchain hybridization<sup>5,6</sup> in TTF-TCNQ will alter the low-frequency dispersion as  $\vec{Q} \rightarrow 0$ , and that our description is also incomplete insofar as it neglects the electron-phonon coupling and the exchange.

For small  $\vec{Q}$  the acoustic mode propagates with

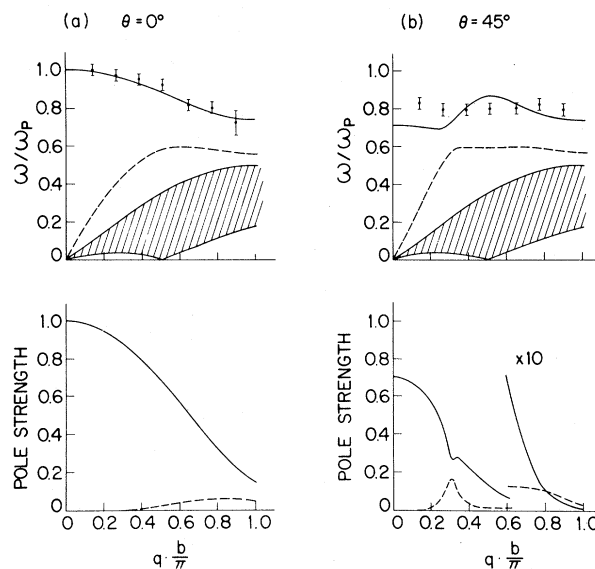


FIG. 1. (a) Plasmon dispersion and expected electron scattering intensities for propagation along the  $b$  axis. Intensities are in units of  $\pi\omega_p/2$ . The shaded area indicates the range of single-particle excitations. Experimental points are from Ref. 1. (b) Same as (a) except for propagation direction in the  $a$ - $b$  plane and making an angle  $45^\circ$  with the  $b$  axis.

velocity

$$v_p = (v_{F1}v_{F2})^{1/2} \left[ 1 + \frac{\omega_p^2}{(v_{F1} + v_{F2})^2} \sum_{\vec{G} \neq 0} \frac{|\beta_1(\vec{G}) - \beta_2(\vec{G})|^2}{|\vec{G}|^2} \right]^{1/2}.$$

The nonlocal screening in our model raises  $v_p$  above both  $v_F$ 's and precludes Landau damping. Since  $v_p < c$ , the acoustic plasmons do not radiate.

To evaluate the importance of the acoustic mode for an electron-scattering experiment like that of Ref. 1, we examine the relevant loss function,<sup>12</sup>  $\text{Im}\epsilon^{-1}(\vec{Q}, \vec{Q}, \omega(\vec{Q}))$ , for the two branches. For  $n=2$  we have from (3) and (1) that

$$\begin{aligned} & \epsilon^{-1}(\vec{Q} + \vec{G}, \vec{Q}_0 + \vec{G}_0, \Omega) \\ &= \frac{\delta_{\vec{Q}, \vec{Q}_0}}{\epsilon_\infty} \left\{ \delta_{\vec{G}, \vec{G}_0} - \frac{4\pi e^2}{\epsilon_\infty |\vec{Q} + \vec{G}|^2 \Delta_2(q, \Omega)} \sum_{i, j \neq i} \beta_i(\vec{Q} + \vec{G}) \chi_i(q, \Omega) [\beta_i^*(\vec{Q}_0 + \vec{G}_0) + \chi_j(q, \Omega) (U_{jj} \beta_i^*(\vec{Q}_0 + \vec{G}_0) \right. \\ & \quad \left. - U_{ij} \beta_j^*(\vec{Q}_0 + \vec{G}_0))] \right\}. \end{aligned} \quad (6)$$

The resulting intensities appear in Fig. 1.

At long wavelengths, the  $\theta=0$  optic and acoustic modes correspond, respectively, to in-phase and  $180^\circ$  out-of-phase charge oscillations on the unlike chains, whereas near the Brillouin zone edge the upper branch becomes purely a strand-1 (TCNQ) excitation and the lower branch purely strand-2 (TTF). Hence the pole strength, which resides entirely in the optic mode and exhausts the  $f$ -sum rule as  $Q \rightarrow 0$ , is more evenly divided between the two branches at the zone edge.

Acoustic plasmons whose energies are smaller than the largest  $W$  can relax into the single-particle continuum via a low-frequency phonon. Together with the weak scattering intensity, the resulting broadening may render the low-frequency part of the acoustic branch experimentally unobservable.

At large  $Q$ , on the other hand, the two branches are on a more nearly equal footing, and both should be detectable. Ritsko *et al.*<sup>1</sup> do not resolve two branches, but do report an anomalous increase in apparent linewidth as the zone edge is approached. Our results for both  $\theta=0^\circ$  and  $\theta=45^\circ$  suggest that at least part of this increase may reflect the growing relative strength of the acoustic mode rather than any increase in relaxation rate. In any event, we agree with the authors of Ref. 1 that plasmon damping in this regime is probably dominated by multipair excitations or (perhaps more likely) the strongly coupled<sup>13</sup> high-frequency intramolecular optical phonons.

At  $\theta=0^\circ$ , our calculated high-frequency plasmon spectrum agrees closely with experiment and displays the negative dispersion expected<sup>3</sup> for  $W$  sufficiently smaller than  $\omega_p$ . Macroscopic

electrodynamics requires that as  $\vec{Q} \rightarrow 0$ , the frequency of the optic branch behaves as  $\omega_p \cos\theta$ , provided that  $\epsilon_\infty$  is isotropic and that no current flows perpendicular to the strands.<sup>3</sup> That the experimental angular dependence<sup>1</sup> is slower than  $\cos\theta$  (cf. Fig. 1) suggests that at least one of these conditions is violated. We neglect the unknown anisotropy of  $\epsilon_\infty$  and consider the effect of a finite interchain bandwidth. The frequency of the optic mode at long wavelengths is now  $\omega^2(Q=0) = \omega_{p\parallel}^2 \cos^2\theta + \omega_{p\perp}^2 \sin^2\theta$ . Expressing the anisotropy in  $\omega_p$  in terms of an anisotropic effective mass, we deduce from the  $\theta=0^\circ$  and  $\theta=45^\circ$  experiments<sup>1</sup> that the anisotropy in the bandwidth is roughly  $W_\perp/W_\parallel \approx (b\omega_{p\perp}/a\omega_{p\parallel})^2 \approx 0.03$  in agreement with band-structure calculations.<sup>5</sup>

The results of Ref. 1 also carry implications for the high-frequency optical conductivity. We underscore the authors' remark that the observation of the lowest-lying well-defined plasmon mode at 0.55 eV places a strict upper limit upon the (lifetime-broadened) effective single-particle bandwidth. Optical experiments,<sup>14</sup> on the other hand, show a small but significant intra-band conductivity persisting to energies at least as large as the first high-frequency absorption threshold near 1 eV. In this region, the simple Drude absorption mechanism clearly cannot obtain. Plausible alternatives include excitations of a single electron-hole pair plus a high-frequency intramolecular optical phonon,<sup>13</sup> or else the optical generation of plasmons via the electron-lattice interaction.<sup>3, 12, 15</sup> In either case, the apparent "Drude" parameters derived at high frequencies need not bear upon the low-frequency conductivity, and inferences about the mechanism

of dc transport drawn from such comparisons<sup>16</sup> must be regarded with caution.

We thank M. A. Butler and J. B. Torrance for useful discussions. P. F. Williams is grateful to Bell Laboratories (Murray Hill, N. J.) and A. N. Bloch to IBM Thomas J. Watson Research Center (Yorktown Heights, N. Y.) for their respective hospitality during part of the time that this work was in progress.

---

\*Work at the Johns Hopkins University supported by the Materials Science Office, Advanced Research Projects Agency, Department of Defense.

†Alfred P. Sloan Foundation Fellow.

<sup>1</sup>J. J. Ritsko, D. J. Sandman, A. J. Epstein, P. C. Gibbons, S. E. Schnatterly, and J. Fields, *Phys. Rev. Lett.* **34**, 1330 (1975).

<sup>2</sup>J. P. Ferraris, D. O. Cowan, V. V. Walatka, and J. H. Perlstein, *J. Am. Chem. Soc.* **95**, 948 (1973).

<sup>3</sup>P. F. Williams and A. N. Bloch, *Phys. Rev. B* **10**, 1097 (1974).

<sup>4</sup>A. N. Bloch, J. P. Ferraris, D. O. Cowan, and T. O. Poehler, *Solid State Commun.* **13**, 753 (1973).

<sup>5</sup>A. J. Berlinsky, J. F. Carolan, and L. Weiler, *Solid State Commun.* **15**, 795 (1974); W. Lee, S. J. Choi,

V. K. S. Shante, A. N. Bloch, D. O. Cowan, and M. H. Cohen, to be published.

<sup>6</sup>M. H. Cohen, J. A. Hertz, P. M. Horn, and V. K. S. Shante, *Int. J. Quantum Chem., Symp.* **8**, 491 (1974); U. Bernstein, P. M. Chaikin, and P. Pincus, *Phys. Rev. Lett.* **34**, 271 (1975).

<sup>7</sup>T. J. Kistenmacher, J. E. Phillips, and D. O. Cowan, *Acta Crystallogr., Sect. B* **30**, 763 (1974).

<sup>8</sup>Here our notation differs slightly from that of Ref. 3, where the subscripts 1 and 2 denote the real and imaginary parts, respectively.

<sup>9</sup>F. Denoyer, R. Comes, A. F. Garito, and A. J. Heeger, to be published.

<sup>10</sup>H. Fröhlich, *J. Phys. C* **1**, 544 (1968).

<sup>11</sup>S.-T. Chui, to be published.

<sup>12</sup>See, for example, E. Foo and J. J. Hopfield, *Phys. Rev.* **173**, 635 (1968).

<sup>13</sup>J. B. Torrance and A. N. Bloch, to be published.

<sup>14</sup>D. B. Tanner, C. S. Jacobsen, A. F. Garito, and A. J. Heeger, *Phys. Rev. Lett.* **32**, 1301 (1974), and **33**, 1559 (1974), and to be published; J. B. Torrance, unpublished work.

<sup>15</sup>P. F. Williams, M. A. Butler, D. L. Rousseau, and A. N. Bloch, *Phys. Rev. B* **10**, 1109 (1974).

<sup>16</sup>P. M. Grant, R. L. Greene, G. C. Wrighton, and A. Castro, *Phys. Rev. Lett.* **31**, 1311 (1973); A. A. Bright, A. F. Garito, and A. J. Heeger, *Solid State Commun.* **13**, 943 (1973).